National Conference on Applied Sciences Synergising the Engineering and Technology
Print ISSN: 2395-6011 | Online ISSN: 2395-602X (www.ijsrst.com)
© 2021 IJSRST | Volume 8 | Issue 2

Preparation, Characterization and Visible light Photocatalytic Activity of Rare earth doped Zinc Oxide Nanoparticles

M. Prathap Kumar[1,2], G. A. Suganya Josephine[3], A. Sivasamy[1*]

[1]Chemical Engineering area, CSIR-Central Leather Research Institute, Adyar, Chennai, Tamil Nadu, India

[2]Department of Chemistry, MVJ College of Engineering, Bangalore, Karnataka, India

[3]AVIT, Vinayaka Mission's Research Foundation, (Deemed to be University) Paiyanoor, Tamil Nadu, India

ABSTRACT

The present study focused on synthesis, characterization and photocatalytic activity of Rare earth doped ZnO nanoparticles for the degradation of Malachite green dye from aqueous phase under visible light irradiation. The concentration of dopant was varied from 3 - 10 wt% and thoroughly characterized by XRD, FT-IR, UV-Vis-DRS, FE-SEM, EDAX and EPR techniques. The band gap energy of (DZ (1:9)) was found to be 3.07 eV, as determined from UV-Vis-DRS analysis. Particle size of the material was in the nano regime (38 to 47 nm) with a hexagonal morphology which is confirmed from FE-SEM analysis. In-situ generation of $OH^{\bullet}$ radicals by light irradiation was confirmed from EPR analysis. The synthesized rare earth doped photocatalyst was investigated under Visible light irradiation for the photocatalytic degradation of non azo dye (MG). At neutral pH (7.10) the photocatalyst displayed 92% degradation of MG dye under both Visible light irradiations. As the substrate concentration increased from 5 ppm to 25 ppm the rate constant showed a decreased trend. The R^2 values clearly indicated that the reaction follows a pseudo-first order kinetics and found to possess enhanced photocatalytic activities under Visible light irradiation. The efficiency and cost effectiveness of DZ (1:9) nanomaterial was determined from reusability studies for the photocatalytic degradation of MG dye and it exhibited better photocatalytic activity even after three cycles of reuse under Visible light irradiation.

Keywords: Rare Earth Doped, Nanoparticles, MG, Visible Light

I. INTRODUCTION

Effluents from various industries such as pharmaceutical, textile, tanneries, paper mills, food, cosmetic industries etc., has been expelled into water bodies thereby contaminating the nature, colour and odour of water. It also affects the natural ecosystem present in water. As the toxic substances exceeds the permissible level it can be harmful and causes serious health disorders to both flora and fauna. The major constituents of effluents includes organic and inorganic compounds, pesticides, heavy metals etc., Several research groups around the world have employed physical and chemical methods for detoxification of pollutants present in waste water. Due to generation and discharge of secondary metabolites and use of solvents etc., (1, 2) the methods were not practised. In order to overcome the disadvantages of these methods Advanced Oxidation Processes (AOP) was employed which has attracted many researchers globally for degradation of organics and

inorganics present in the waste water in the presence of semiconductor photocatalyst. Semiconductor metal oxides are suitable candidates for light induced photocatalytic processes (3, 4). Metal oxides such as TiO2, ZnO, Bi2O3, WO3, CeO2 etc., exhibits excellent photocatalytic activity in degradation of organic and inorganic molecules (5, 6, 7, 8). Since UV light is energy intensive and the availability is less, hence we focused on synthesis of visible light active photocatalyst by modification of band gap. This is achieved by doping of metals, non-metals, rare earth metals etc., (9, 10, 11, 12, 13, 14).

In the present work we focused on visible light active Dy doped ZnO by co-precipitation technique. The prepared material was characterised by FT-IR, XRD, UV-Vis-DRS, FE-SEM, EDAX and EPR techniques. Evaluation of the photocatalyst was investigated by degradation of MG dye under Visible light irradiation.

II. METHODS AND MATERIAL

2.1 Materials

Dysprosium Nitrate hexahydrate (99.9%, Dy(NO3).6H2O), Zinc nitrate hexahydrate (98%, Zn(NO3)2•6H2O) and DMPO (5,5-Dimethyl-1-pyrroline-N-Oxide) were purchased from Sigma-Aldrich, India. Na2CO3, Orange G dye (90%, 7-hydroxy-8-phenlyazo-1,3-naphthalenedisulfonic acid disodium salt) and Malachite green dye (90%, 4-{[4-(Dimethylamino) phenyl] (phenyl) methylidene}-N,N-dimethylcyclohexa-2,5-dien-1-iminium chloride) were supplied by S.D. Fine Chem., Mumbai, India.

2.2 Preparation of Dy3+ doped ZnO (DZ)

The rare earth doped ZnO used in this study was prepared by a simple co-precipitation technique as reported elsewhere (15). A typical procedure involves ZnNO3.6H2O and DyNO3.6H2O mixed in the required molar ratio in double distilled water and Na2CO3 was prepared in a 1:1 ratio with respect to the nitrates. The salt solution was vigorously stirred followed by dropwise addition of Na2CO3 which resulted in the formation of white precipitate. After successful addition of Na2CO3, the obtained precipitate was allowed to stir for 15 min, filtered, washed thrice with water and then with ethanol. The obtained precipitate was dried at 100°C in an oven overnight and then calcined at 700°C for 2 h. The various doping ratios prepared were: 0:100, 3:97, 5:95, 7:93, 10:90, 100:0 of dysprosium nitrate : zinc nitrate and named as PZ (pristine ZnO), 3DZ, 5DZ, 7DZ, 10DZ, PD (pristine Dy2O3).

2.3 Instrumental Analysis

The instrumental techniques such as X-ray diffraction (XRD) analysis, Fourier transform-infra red (FT-IR), ultra-violet diffuse reflectance spectroscopy (UV-DRS), field emission scanning electron microscope (FE-SEM), energy dispersive X-ray diffraction (EDAX) and (EPR) spectroscopy were employed for characterization of prepared semiconductor material. The bond stretching vibrational frequencies of metal oxides were determined by FT-IR analysis in a Perkin Elmer instrument. Crystallinity and phase analysis was determined from X-ray diffraction by PAN analytical X-ray diffractometer, Germany, with scanning angle 2θ in the scan range between 10◦ and 70◦ with Cu Kα radiation. In order to determine the surface morphology and particle size of the synthesized material FE-SEM (Model Supra 55 - Carl Zeiss, Germany) was carried out. EDAX analysis was

carried out to determine the percentage of dopant concentration in the synthesized material. UV-Diffuse Reflectance Spectroscopy (UV 2600, Shimadzu spectrometer; Japan) was employed to calculate the band-gap energy of the nanomaterial with a scan speed of 200 nm/min in the UV-Visible range (200-800nm). EPR spectrometer (Model - Bruker EMX X Band) was employed to determine the generation of OH• radicals in the in-situ process of Visible irradiation.

2.4 Photocatalytic degradation studies

Malachite Green (MG) dye was employed as model pollutant for the photocatalytic degradation Visible light irradiations. The photocatalytic degradation was performed in an annular type photoreactor (Heber Scientific Company Ltd., Chennai, India) with an irradiation source of 500 W tungsten halogen lamp. The irradiation source was surrounded by a water jacketed tube which was cooled continuously with water circulation to reduce the heat. Preliminary experimental parameters like effect of pH, catalyst dosage and substrate concentration were performed to determine the optimal dopant concentration that exhibits enhanced photocatalytic activity with respect to the undoped material. The reaction tubes containing the aqueous dye solution and photocatalyst were irradiated for a specific time and kinetic analysis was conducted by withdrawing aliquots of the samples at prescribed time intervals to assess the extent of degradation process by UV-visible absorption measurements. The substrate concentration before and after photocatalytic degradation was computed from a calibration curve and the percentage degradation of MG was calculated using equation (1).

degradation efficiency (%) = (C0-Ce/ C0) * 100 (1)

where, C0 and Ce are the initial and final MG dye concentrations in the aqueous phase, respectively.

III. RESULTS AND DISCUSSION

3.1 FT-IR analysis

The FT-IR spectra of synthesized (DZ) material is shown in Fig. 1(a). The bond stretching frequencies of metal to oxygen bond i.e., Dy-O and Zn-O was observed at 481 and 533 cm^{-1} respectively of the photocatalyst confirming the composition of the prepared material [16, 17].

3.2 X-Ray Diffraction Pattern

The XRD patterns of DZ photocatalyst is shown in **Fig. 1(b).** The material exhibited crystalline nature which is confirmed from clear and sharp peaks and the patterns obtained were matched with zinc oxide and dysprosium oxide JCPDS data (ZnO-JCPDS No. 36-1451 and Dy2O3-JCPDS 01-079-1722) (18). The as-prepared DZ photocatalyst exhibited (222) reflection which is a characteristic of Dy_2O_3 confirming the presence of Dy^{3+} in the photocatalyst. The average crystallite size of the prepared material was calculated using Scherer equation eq (2).

$$D = k\lambda / (B \cos \theta) \quad (2)$$

where, k is 0.94 (spherical nanoparticles), λ the wavelength of radiation (0.154 nm) and B is the full width at half maximum (FWHM) and θ half the diffraction angle. The average crystallite size of DZ photocatalyst was found to be 36.36 nm. 10DZ exhibited diffraction planes at (222), (100), (400), (002), (101), (102), (110), (103), (004), (112) and (201). The lattice parameters 'a' and cell volume 'c' of DZ photocatalyst was found to be 1.0625 and 1.1935 nm respectively.

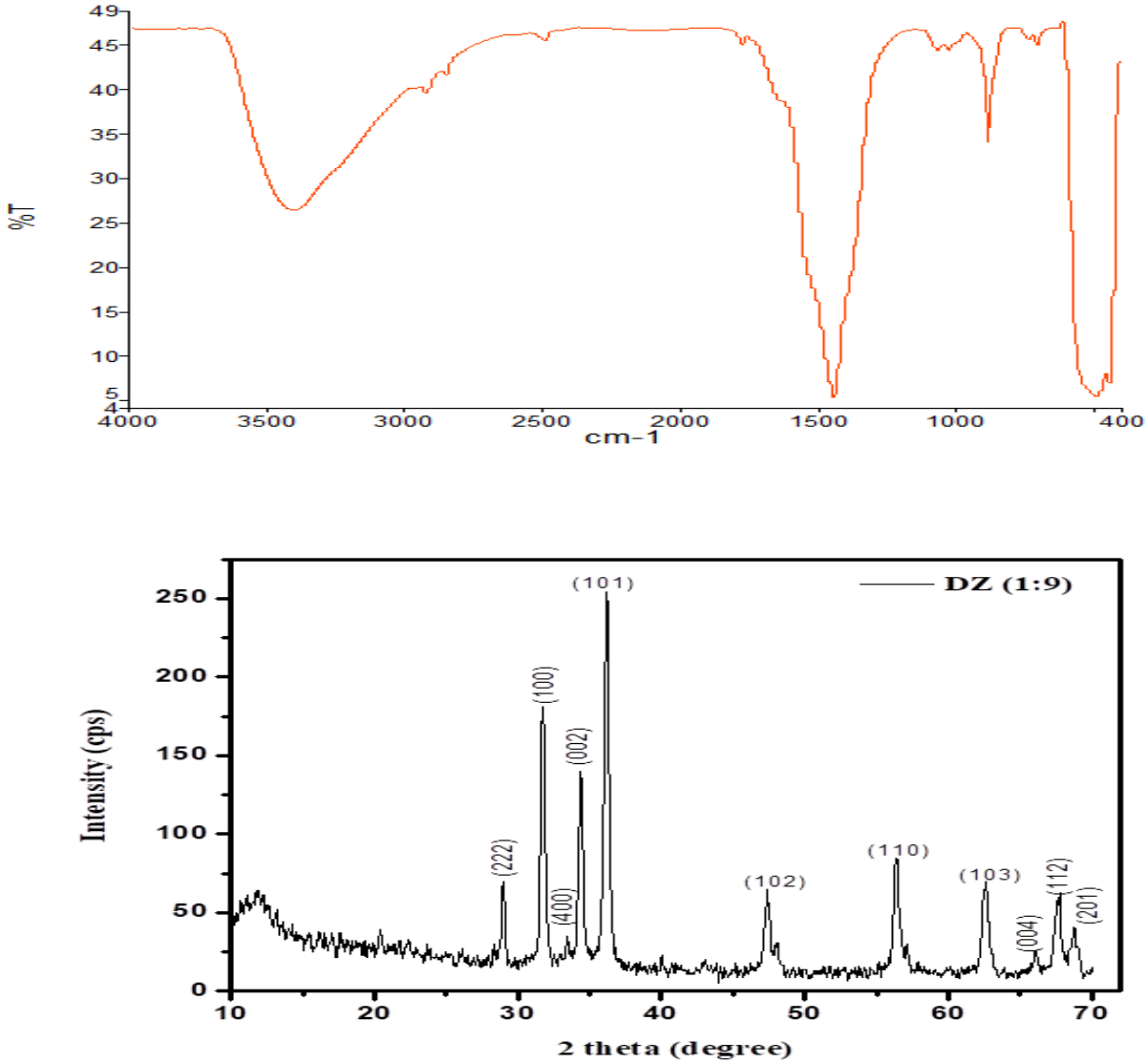

Fig. 1. (a) FT-IR spectrum and; (b) X-ray Diffraction pattern of DZ (1:9) photocatalyst

3.3 UV- Vis Diffuse Reflectance Spectrum

The band gap energy (E_g) of prepared nanomaterial was determined by UV- Vis DRS spectrometer and the spectrum was recorded for PZ, 3 DZ, 5 DZ, 7 DZ and 10 DZ and is shown in **Fig. 2(a) and (b).** As the doping concentration of Dy^{3+} increases from 0-10% a shift towards the visible region was observed. The absorption bands of lanthanide elements was observed above 700 nm and is due to f-f transitions. A plot of $(Ahv)^2$ *vs* hv gives the band gap energy (Eg) of the prepared photocatalyst and is found to be 3.16 eV for PZ and 3.07 eV for 10 DZ respectively.

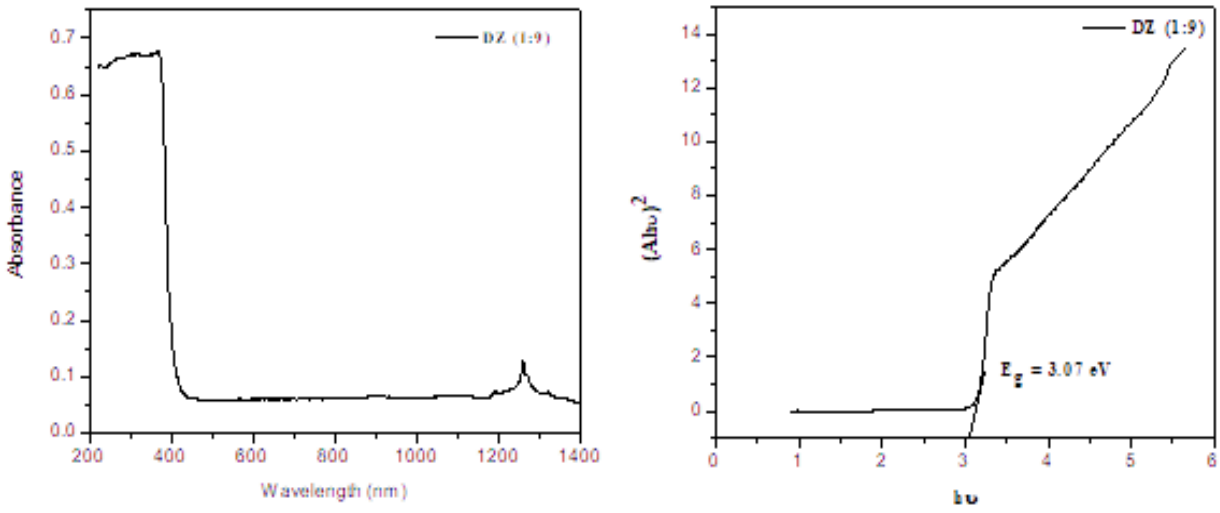

Fig. 2. (a) UV-Vis DRS pattern and; (b) Band gap energy of DZ (1:9) photocatalyst

3.4 Morphology and surface roughness

Surface morphology and particle size of the as-prepared material was determined by FE-SEM analyses and the results are displayed in **Fig. 3.** It exhibits hexagonal morphology with particle size ranging from 38 - 47 nm as shown in **Fig. 3(a)**. EDAX analysis was carried out to determine the elemental composition of the prepared material and confirms the presence of Zn, Dy and O elements and is shown in **Fig. 3(b)**.

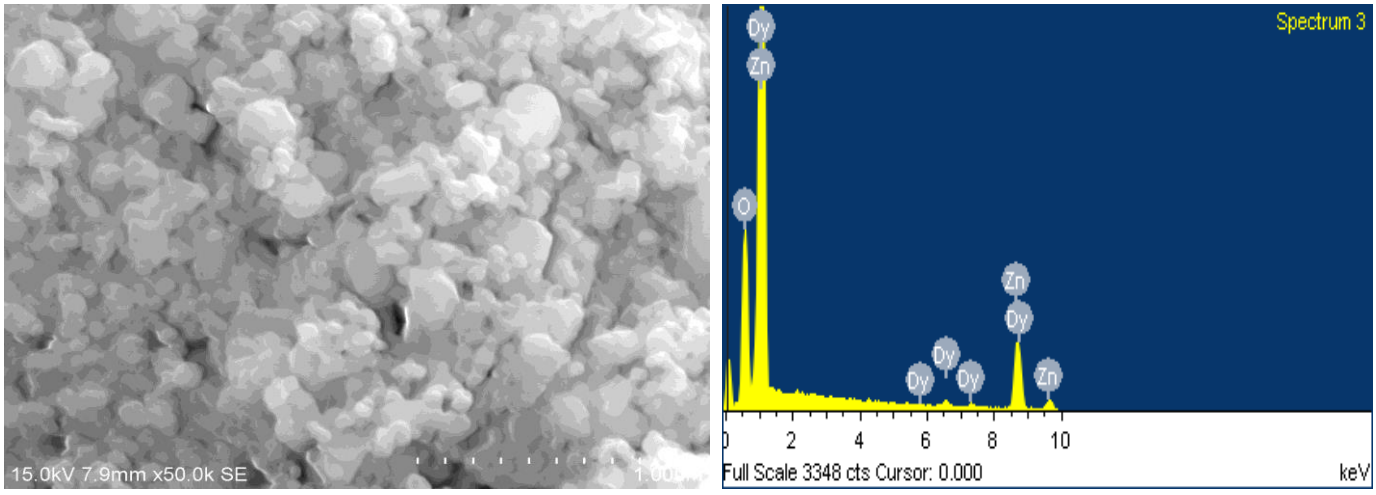

Fig. 3. Morphological and Elemental composition by (a) FESEM; (b) EDAX; and (c) HRTEM analysis

3.5 EPR studies

EPR spin trap technique was employed to probe the reactive oxygen species generated on the surface of DZ photocatalyst upon Visible light irradiation. The spin trapping agent employed was DMPO. As shown in Fig.4 four characteristic peaks in the ratio of 1:2:2:1 was observed indicating the spin trapped DMPO-OH•. This clearly shows that OH• radicals were generated on the surface of DZ photocatalyst.

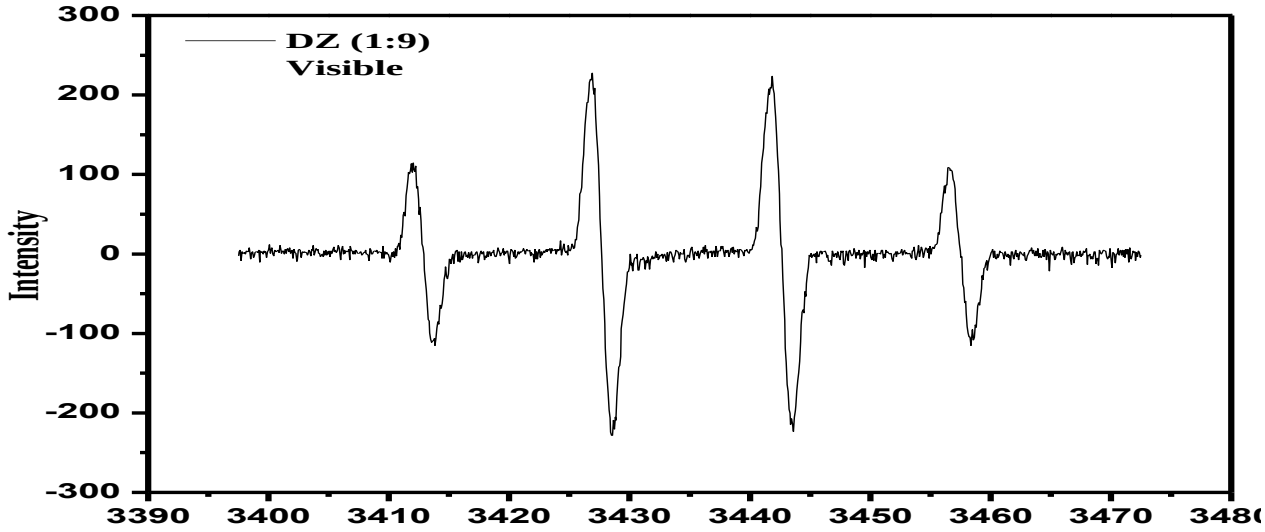

Fig. 4. EPR spectrum of the DMPO spin trapped •OH radical generated *in-situ* under (a) visible irradiation.

3.6 Preliminary experimental parameters for photocatalytic degradation of Malachite Green dye molecules under Visible light irradiation

3.6.1 Effect of aqueous phase pH

Effect of aqueous phase pH on photocatalytic degradation of MG dye by DZ photocatalyst under Visible light irradiation was performed. A series of aqueous phase pH of the dye solutions varying from 2 - 11 were prepared and irradiated. 10 mg of DZ photocatalyst in 10 ppm/10 ml of MG dye concentration exhibited more than 90% of degradation under Visible light irradiation at neutral pH and the result is shown in Fig. 5 (a).

3.6.2 Effect of catalyst dosage

To determine the optimum dosage of catalyst required for photocatalytic reaction, studies on varying catalyst dosage were carried out and the results are shown in Fig. 5 (b). The catalyst dosage was varied from 5 - 25 mg/ 10 ml of 10 ppm MG dye concentration. It was observed that 10 mg of DZ photocatalyst exhibited 97% degradation under Visible light irradiation. The percentage of degradation decreased on increasing the dosage of catalyst. This is due to large amount of catalyst present in the system and causing more turbidity and that obstructs the photons entering onto the surface of the catalyst thereby reduces the photocatalytic activity of the catalysts.

3.6.3 Effect of substrate concentration

The effect of varying initial dye concentration on photocatalytic degradation of MG dye molecules DZ photocatalyst under Visible light irradiations was investigated to determine the optimum concentration of MG dye molecules required for further photocatalytic reaction. The substrate concentration was varied from 5 to 25 mg/l for 10 ml of test solutions. 10 mg of DZ photocatalyst exhibited above 98% of degradation for 10 ppm of MG dye molecules under Visible light irradiations at neutral pH. The percentage degradation decreased from 96% (5 ppm) to 95% (25 ppm) was observed for MG dye and the obtained results were shown in Fig. 5 (c). As the substrate concentration increased decrease in percentage of degradation was observed and is due to

reduction in number of photons reaching the surface of catalyst which further results in lack of hydroxyl radicals.

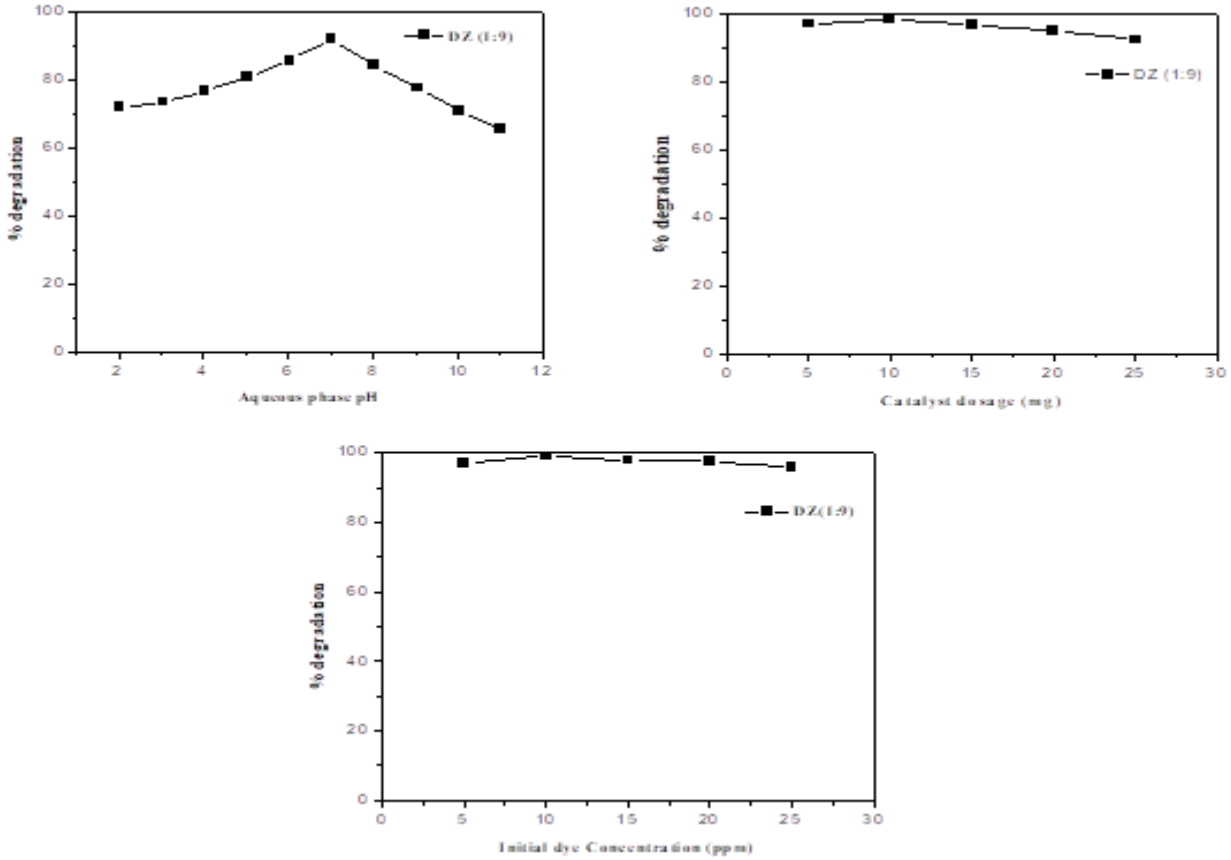

Fig. 5 Preliminary photocatalytic studies of the prepared 10 DZ photocatalyst under Visible light irradiation (a) Effect of pH, (b) Variation of photocatalyst mass and (c) Variation of substrate concentration

3.6.4 Kinetics

The kinetics of photodegradation of MG dye molecules by DZ photocatalyst was monitored by time dependence studies. The kinetic experiments were performed for various initial substrate concentrations such as 5, 10, 15, 20 and 25 ppm with catalyst dosage of 100 mg of DZ photocatalyst in 100ml of preferred dye concentration. Samples were withdrawn at regular intervals of time during the photocatalytic experiments and absorbance were measured at respective λmax of the dye molecule. The residual concentrations were computed from the calibration graph and COD levels were analyzed. DZ photocatalyst exhibited 89% of degradation at 240 min under Visible light irradiation. The obtained results were tabulated in Table 1 and Fig. 6 (a). The pseudo-first order rate constant were calculated and the values were found to decrease as shown in Table 1. The R2 values clearly indicated that the reaction follows pseudo-first order kinetics for photocatalytic degradation of MG dye molecules which is shown Fig. 6 (b). A decrease in COD level from 584 mg/L to 14.4 mg/L was observed for MG dye degradation under Visible light irradiation and results are shown in Fig. 6(c).

Table 1.

Malachite green (Visible light irradiation)					
Catalyst	DZ				
Concentration of the organic molecule (ppm)	5	10	15	20	25
Rate Constant x 10^{-3} min^{-1}	12.71	9.68	6.97	5.70	5.41
R^2	0.9875	0.9811	0.9822	0.9931	0.9885
% COD removal	95.00	97.53	93.85	74.59	72.39

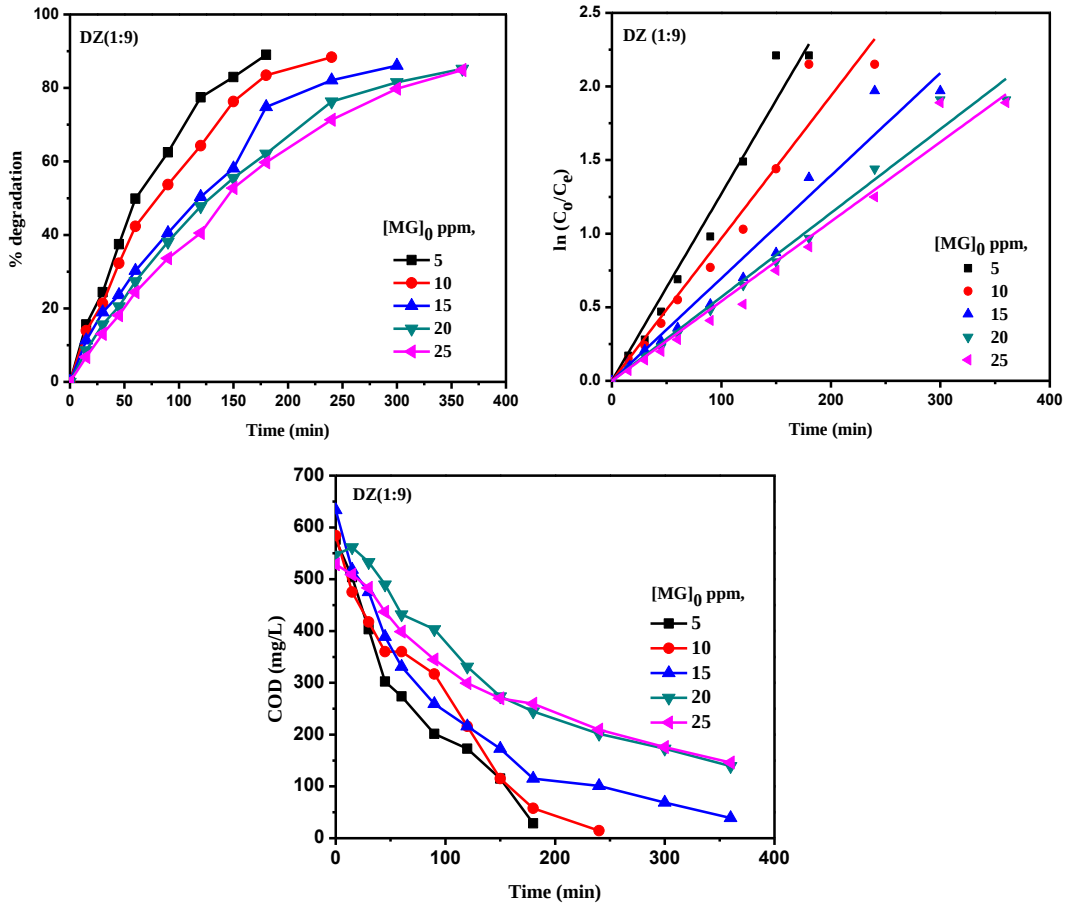

Fig. 6. (i) Kinetics of photo degradation of MG dye molecule (ii) Pseudo- first order kinetic plots for photo degradation of MG dye molecule (iii) COD removal under Visible light irradiation.

3.6.5 Effect of Electrolytes

The interference of inorganic anions present in the industrial waste water on photocatalytic degradation of MG dye molecules by DZ (1:9) photocatalyst under Visible light irradiation was investigated. The electrolytes employed were KCl, $MgSO_4$, Na_2CO_3 and $NaHCO_3$. The electrolyte concentrations were varied from 1 to 7 wt% for dye molecules. The obtained results were shown in Fig. 10. As the concentration of KCl is increased, the percentage of degradation of MG dye molecules decreases and is due to chloride ions that acts as radical scavengers (19). It is confirmed that carbonates and bicarbonates has no effect on the activity. Similarly,

increasing the concentration of sulphate up to 1.5% showed an increase in photocatalytic degradation and is due to generation of sulphate radicals in the photocatalytic system. Further increasing the concentration of sulphate beyond 1.5% leads to decreased photocatalytic degradation of MG dye molecules. This phenomena may be due to adsorption of sulphate radicals on the surface of the catalyst which competes with the substrate molecules (20).

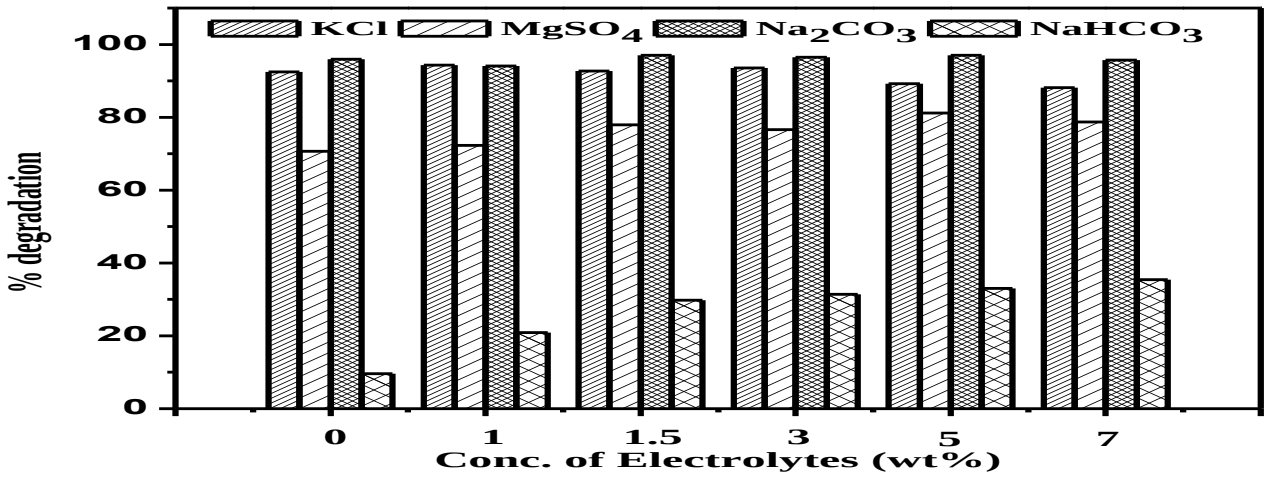

Fig. 8. Effect of electrolytes on the photocatalytic degradation MG dye molecule by 10DZ under Visible light irradiation

3.6.6 Reusability Studies

The efficiency of the DZ photocatalyst was determined from reusability studies in photocatalytic degradation of MG dye molecule under Visible light irradiation and the results were shown in Fig. 11. DZ (1:9) photocatalyst shows decrease in percentage of degradation from 93% to 88% under Visible light irradiation indicating that the catalyst retains its photocatalytic activity even after three cycles of regeneration.

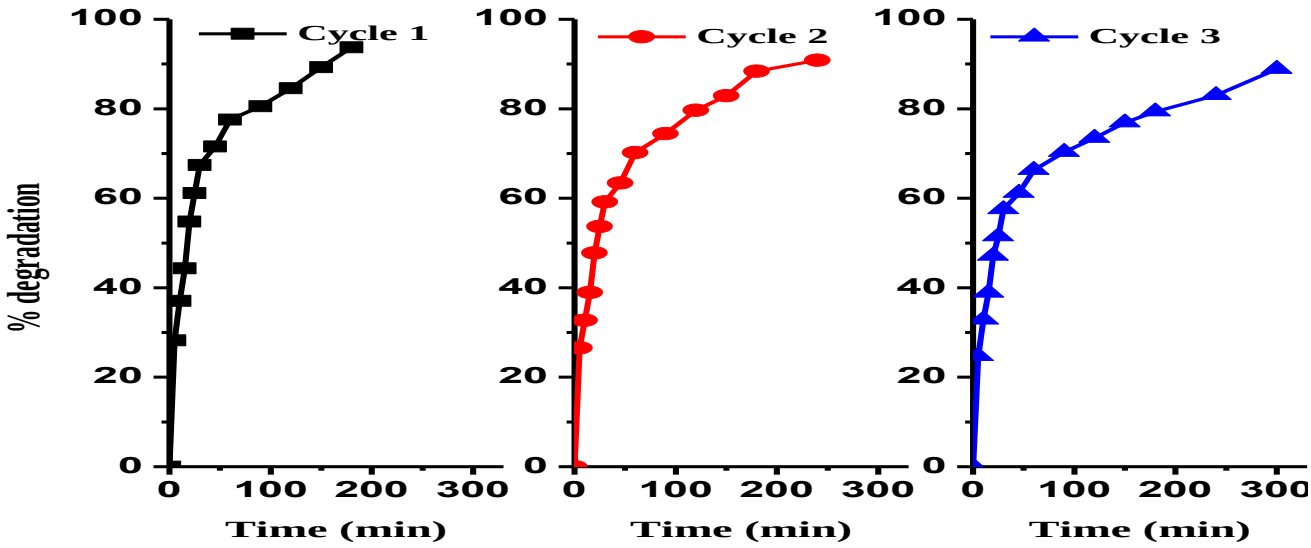

Fig. 9 Reusability studies of 10DZ in photocatalytic degradation of MG dye molecule under (i) Visible light irradiation.

3.6.7 By- Product analysis

The UV-Visible absorbance spectrum further supports that the MG dye molecule has completely degraded and no peaks corresponding to UV-Visible active by-products are present from 200 - 800 nm in the spectrum. Hence, the prepared photocatalyst completely degrades the MG dye molecule effectively under Visible light irradiation. The Fig. shows the change in colour on irradiation of MG dye molecule in the presence of the 10 DZ photocatalyst.

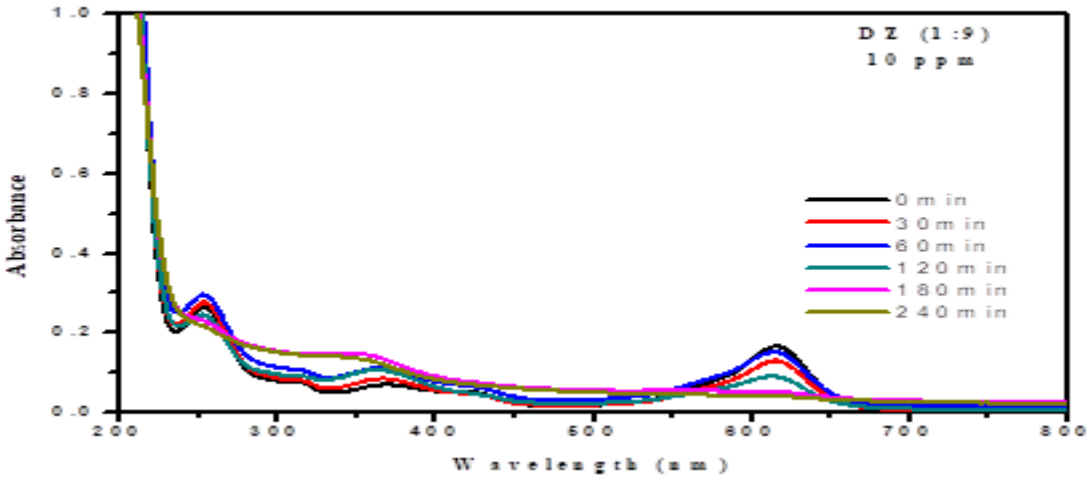

Fig. 10 UV- Visible absorbance spectrum of MG dye molecule under Visible light irradiation

IV. CONCLUSION

Nanocrystalline dysprosium modified ZnO (DZ) photocatalyst prepared by co-precipitation method and characterized by FT-IR, XRD, UV-Vis-DRS, FE-SEM, EDAX & EPR techniques. The characterization results of the synthesized photocatalyst clearly confirms the presence of elements, band gap, crystallinity, morphology & EPR analysis confirms the generation of ·OH radicals in photocatalytic system. The synthesized photocatalyst was evaluated for its photocatalytic activity in degradation of Malachite Green dye molecules in aqueous phase under Visible light Irradiations. Preliminary studies like effect of pH, varying catalyst dosage and variation of initial substrate concentration were studied in detail. Kinetics studies were investigated and the reaction followed pseudo-first order relationship. The progress of the reaction was also monitored by COD analysis. The efficiency of the photocatalyst was determined from reusability studies. Rare earth doped metal oxides exhibited better photocatalytic activity than Pristine metal oxides.

V. REFERENCES

[1]. C. Philippe, B. Vandevivere, V. Willy, J. Chem. Technol. Biotechnol. 72 (1998) 289,
[2]. Y.M. Slokar, M.A. Le Marechal, Dyes Pigm. 37 (1998) 335
[3]. Hoffmann, M. R.; Martin, S. T.; Choi, W. Y.; Bahnemann, D. W. Environmental Applications of Semiconductor Photocatalysis. Chem. Rev. 1995, 95, 69–96,

[4]. Teoh, W. Y.; Scott, J. A.; Amal, R. Progress in Heterogeneous Photocatalysis: From Classical Radical Chemistry to Engineering Nanomaterials and Solar Reactors. J. Phys. Chem. Lett. 2012, 3, 629–639
[5]. D. Devilliers, Energeia 17 (2006) 1–6,
[6]. M.M. Khan, S.A. Ansari, D. Pradhan, M.O. Ansari, D.H. Han, J. Lee, M.H. Cho, J. Mater. Chem. A 2 (2014) 637–644,
[7]. S.A. Ansari, M.M. Khan, M.O. Ansari, J. Lee, M.H. Cho, New J. Chem. 38 (2014) 2462–2469,
[8]. S. Anandan, M. Miyauchi, Chem. Commun. 48 (2012) 4323–4325
[9]. S.A. Ansari, M.M. Khan, S. Kalathil, A.N. Khan, J. Lee, M.H. Cho, Nanoscale 5 (2013) 9238–9246,
[10]. Z. Ambrus, N. Balazs, T. Alapi, G. Wittmann, P. Sipos, A. Dombi, K. Mogyorosi, Appl. Catal. B: Environ. 81 (2008) 27–37,
[11]. S.A. Ansari, M.M. Khan, J. Lee, M.H. Cho, J. Ind. Eng. Chem. 20 (2014) 1602–1607,
[12]. T.A. Egerton, J.A. Mattinson, J. Photochem. Photobiol. A: Chem. 194 (2008) 283–289,
[13]. S.A. Ansari, M.M. Khan, M.O. Ansari, J. Lee, M.H. Cho, J. Phys. Chem. C 117 (2013) 27023–27030,
[14]. K.G. Kanade, B.B. Kale, J.O. Baeg, S.M. Lee, C.W. Lee, S.J. Moon, H. Chang, Mater. Chem. Phys. 102 (2007) 98–104
[15]. Anandana, S., Vinua, A., Mori, T., Gokulakrishnan, N., Srinivasu, P., Murugesan, V., Ariga, K., 2007. Photocatalytic degradation of 2,4,6-trichlorophenol using lanthanum doped ZnO in aqueous suspension. Catal. Commun.: 8, 1377-1382
[16]. R.Y. Hong, J.H. Li, L.L. Chen, D.Q. Liu, H.Z. Li, Y. Zheng, J. Ding, Synthesis, surface modification and photocatalytic property of ZnO nanoparticles, Powder Technol. 189 (2009) 426-432,
[17]. Y. Zhang, K.L. Zhang, M.K. Jia, H. Tang, J.T. Sun, L.J. Yuan, Synthesis, Characterization of a Novel Compound SnEr2O4, Chin. Chem. Lett. 13 (2002) 587-589
[18]. B. Karthikeyan, C.S. Suchand Sandeep, T. Pandiyarajan, P. Venkatesan, P. Reji, Spectrally broadened excitonic absorption and enhanced optical nonlinearities in Dy3+-doped ZnO nanoparticles, Appl. Phys. A: Mater. Sci. Process. 102 (2011) 115-120
[19]. Trabelsi, H.; Atheba, P.; Gbassi, G. K.; Ksibi, M.; Drogui, P. Int. J. Hazard. Mater. 2012, 1, 6-10
[20]. Sakthivel, S.; Neppolian, B.; Shankar, M. V.; Arabindoo, B.; Palanichamy, M.; Murugesan, V. Sol. Energy Mater. Sol. Cells 2003, 77, 65–82